



# *In silico* analysis of ACE2 orthologues to predict animal host range with high susceptibility to SARS-CoV-2

El Mehdi Bouricha<sup>1</sup> · Mohammed Hakmi<sup>1</sup> · Jihane Akachar<sup>1</sup> · Lahcen Belyamani<sup>2</sup> · Azeddine Ibrahim<sup>1</sup>

Received: 22 June 2020 / Accepted: 7 October 2020 / Published online: 21 October 2020  
© King Abdulaziz City for Science and Technology 2020

## Abstract

SARS-CoV-2, which causes severe pneumonia epidemics, probably originated from Chinese horseshoe bats, but the intermediate and host range is still unknown. ACE2 is the entry receptor for SARS-CoV-2. The binding capacity of SARS-CoV-2 spike protein to ACE2 is the critical determinant of viral host range and cross-species infection. Here, we used an *in silico* approach to predict the potential animals range with high susceptibility to SARS-CoV-2 by modelling and studying the Spike–ACE2 interaction of 22 domestic and wild animals. Our results showed that all studied animals are potentially susceptible to SARS-CoV-2 infection with a slight difference in the binding affinity and stability of their ACE2–RBD complexes. Furthermore, we identified a specific substitution of tyrosine to histidine at position 41 in ACE2 that likely reduces the affinity to SARS-CoV-2 in horses and greater horseshoe bats. These results may help to provide important insights into SARS-CoV-2 host range which will make it possible to control the spread of the virus and identify animal models that could be used for screening antiviral drugs or vaccine candidates against SARS-CoV-2.

**Keywords** ACE2 orthologues · COVID-19 · SARS-CoV-2 susceptibility · Host range

## Introduction

Coronaviruses (CoVs) are members of the family Coronaviridae in the Nidovirales order. These viruses can infect a broad range of animals as well as humans, resulting in mild, common cold-like symptoms (Peiris 2012). Nevertheless, three deadly CoV epidemics have already occurred in the twenty-first century, including severe acute respiratory syndrome (SARS), Middle East respiratory syndrome (MERS) and the current COVID-19 outbreak. All of them involve emerging pathogenic CoVs, originated in animals and subsequently transmitted to humans (Fehr and Perlman 2015; Zhou et al. 2020).

Phylogenetic studies indicate that SARS-CoV, MERS-CoV and SARS-CoV-2 are zoonotic pathogens that probably

evolved from bats and were transmitted to humans through intermediate hosts which are the palm civets for SARS-CoV and camels for MERS-CoV (Zhou et al. 2020; Cui, Li, and Shi 2019). However, the intermediate host of SARS CoV-2 has not yet been identified (Liu et al. 2020).

Coronaviruses comprise four structural proteins, including envelope (*E*), membrane (*M*), nucleocapsid (*N*) and spike (*S*) proteins (Du et al. 2016; Wang et al. 2020). The latter one plays a critical role in viral attachment, fusion and entry into host cells to cause the final infection (Wang et al. 2020). S protein contains two functional subunits, S1 and S2. The S1 subunit contains a receptor-binding domain (RBD) that recognise and bind to the host cell receptor, while the S2 subunit is responsible of the cellular and viral membranes fusion (Kirchdoerfer et al. 2016; Yuan et al. 2017; Song et al. 2018).

The specificity of the interaction between the virus and its host cell receptor(s) is the first step in triggering a viral infection and is a key determinant of host cells and species range (Douam et al. 2015). In SARS-CoV-2, angiotensin-converting enzyme 2 (ACE2) was reported as the main host cell receptor that allows its entry (Zhou et al. 2020). This entry involves the recognition and direct binding of the virus to ACE2 receptor via RBD of spike protein, then fusion of

✉ Azeddine Ibrahim  
a.ibrahimi@um5s.net

<sup>1</sup> Medical Biotechnology Laboratory (MedBiotech), Rabat Medical and Pharmacy School, Mohammed Vth University in Rabat, Rabat, Morocco

<sup>2</sup> Emergency Department, Military Hospital Mohammed V, Rabat Medical and Pharmacy School, Mohammed Vth University in Rabat, Rabat, Morocco

the virus and host cell membrane through the S2 subunit (Walls et al. 2020). ACE2 is expressed in most mammals; however, not all ACE2s can be used by SARS-CoV-2 as entry receptors (Qiu et al. 2020).

In this study, we used an *in silico* approach to model the ACE2/SARS-CoV-2-RBD interaction from 22 mammals including forest, livestock and domestic animals to predict those that are highly susceptible to SARS-CoV-2 which could be monitored to prevent future outbreaks since the precise host tropism of SARS-CoV-2 remains unclear.

## Methods

### Identification of putative orthologues of human ACE2 protein and sequences selection

Human ACE2 (hACE2) orthologue proteins were identified by an NCBI blast search against non-redundant protein sequences database using the UniProt “Q9BYF1” accession number as query sequence. All hits with an identity above 97% and coverage above 98% were selected, representing a set of five species which are: *Gorilla gorilla gorilla* (XP\_018874749.1), *Pan paniscus* (XP\_008972428.1), *Pongo abelii* (XP\_024096013.1), *Hylobates moloch* (XP\_032612508.1) and *Nomascus leucogenys* (XP\_003261132.2). Additionally, 16 protein sequences (with identity > 80% and coverage > 98%) of forest, livestock and domestic mammals were added. These sequences are as follows: *Mesocricetus auratus* (XP\_005074266.1), *Phodopus campbelli* (ACT66274.1), *Ovis aries* (XP\_011961657.1), *Oryctolagus cuniculus* (ACT66271.1), *Panthera tigris altaica* (XP\_007090142.1), *Felis catus* (XP\_023104564.1), *Canis lupus familiaris* (XP\_005641049.1), *Canis lupus dingo* (XP\_025292925.1), *Vicugna pacos* (XP\_006212709.1), *Sus scrofa domesticus* (ACT66265.1), *Camelus dromedarius* (KAB1253106.1), *Equus przewalskii* (XP\_008542995.1), *Equus caballus* (XP\_001490241.1), *Rhinolophus macrotis* (ADN93471.1), *Rhinolophus sinicus* (ADN93475.1), *Rhinolophus ferrum-equinum* (BAH02663.1).

### Phylogenetic analysis

Multiple sequence alignment of the selected sequences was done using Clustal Omega available in Jalview (Sievers et al. 2011; A. M. Waterhouse et al. 2009), and phylogenetic tree was constructed by MEGA X using JTT model of maximum likelihood method with 5000 bootstrap replicates (Kumar et al. 2018). Furthermore, based on the known key residues implicated in hACE2/SARS-CoV-2-RBD interaction reported from previous studies, we analysed whether these residues were conserved or changed in ACE2 across species.

### Homology modelling of ACE2–RBD complexes

3D structures of orthologous ACE2 in complex with SARS-CoV-2-RBD were built using SWISS-MODEL workspace (A. Waterhouse et al. 2018). For each model, the sequences of the target ACE2 and RBD were used as hetero inputs and the structure 6M0J as template. The quality of the built models was analysed using the structure assessment tool in SWISS-MODEL workspace. The obtained models were further processed in UCSF chimera 1.14 (Pettersen et al. 2004) by adding hydrogen atoms and performing 2500 steps of steepest descent and 2500 steps of conjugate gradient minimizations to relax the structures and remove any possible clashes. The visualisation of complexes was performed using free Maestro (Maestro, Schrödinger, 2020).

### Binding affinity estimation and hotspots prediction

The prediction of binding affinity was performed for all modelled complexes using PRODIGY (PROtein binDING enerGY prediction) web services (Xue et al. 2016) and the prediction of hotspots at ACE2/SARS-CoV-2-RBD interface was done using SpotOn web server (Moreira et al. 2017).

### Molecular dynamics simulation

Molecular dynamics (MD) simulation was used to explore the stability of the ACE2–RBD complexes of the studied species. The solvated systems of ACE2–RBD complexes of each species were built using the solvate plugin in VMD 1.9.3 (Humphrey, Dalke, and Schulten 1996) using the TIP3P water model. The box size was set to “use molecule dimensions” and box padding was set to 10 Å. The systems were neutralized by sodium (Na<sup>+</sup>) and chloride ions (Cl<sup>−</sup>) using the Autoionize plugin and the generated model systems were exported in Maestro (.mae) file format. Each system was simulated independently for 10 ns with a 10 ps recording interval using Desmond (Bowers et al. 2006) in NPT ensemble at a constant temperature of 300 K and 1.01325 bar pressure.

## Results

### Multiple sequence alignment of ACE2 orthologues

As reported from the previous structural studies, 15 key residues in hACE2 could be involved in the surface interaction between the hACE2 and RBD–Spike protein (Lan et al. 2020; Yan et al. 2020; Shang et al. 2020). Among them, the two lysines at position 31 and 353 are the most critical

residues for RBD recognition (Shang et al. 2020). Multiple sequence alignment was performed in the present work, to compare the conservation of these key amino acids across ACE2 proteins from the 22 selected species. As shown in Table 1, *Gorilla gorilla gorilla*, *Pan paniscus*, *Pongo abelii*, *Hylobates moloch* and *Nomascus leucogenys*, which have a homology more than 97%, show a complete similarity to the 15 key residues of hACE2, while *Rhinolophus ferrumequinum* shows a low similarity with only 7 conserved residues followed by *Rhinolophus sinicus*, *Rhinolophus macrotis*, *Equus caballus* and *Equus przewalskii* with 6 conserved residues.

### Binding energy estimation, molecular dynamics simulation and hotspot prediction of ACE2/SARS-CoV-2-RBD complexes

Homology modelling of ACE2–RBD complexes was performed to provide an insight into the interaction mode, binding affinity and hotspot residues of each generated

interaction complex between orthologous ACE2 and SARS-CoV-2-RBD. Commonly, the affinity of an interaction is described through the equilibrium dissociation constant (Kd) or, in thermodynamic terms, the Gibbs free energy ( $\Delta G$ ) where the lowest Kd or  $\Delta G$  value corresponds to high binding affinity (Vangone and Bonvin 2015). As shown in the Table 2, ACE2/SARS-CoV-2-RBD interaction of *Rhinolophus ferrumequinum* shows the highest Kd values (14 nM), followed by *Equus caballus* and *Equus przewalskii* with a Kd value of 6.1 nM, while the Kd value of *Canis lupus familiaris*, *Panthera tigris altaica*, *Camelus dromedarius*, *Canis lupus dingo*, *Felis catus* and *Phodopus campbelli* fall below 2 nM. The others species had a Kd value ranging between 2.2 nM and 3.8 nM. On the other hand, compared to humans (*Homo sapiens*), the majority of species showed equal or more favourable affinity. Furthermore, MD simulations were performed for nine species including: three species with high affinity (*Canis lupus familiaris*, *Panthera tigris altaica* and *Camelus dromedarius*), three species with low affinity (*Equus caballus*, *Equus przewalskii* and

**Table 1** Alignment of critical contacting residues between SARS-CoV-2-RBD and ACE2 from different species

Species	24	30	31	34	35	37	38	41	42	79	82	83	353	357	393	Matched amino acids
<i>Homo sapiens</i>	Q	D	K	H	E	E	D	Y	Q	L	M	Y	K	D	R	15
<i>Nomascus leucogenys</i>	Q	D	K	H	E	E	D	Y	Q	L	M	Y	K	D	R	15
<i>Pan paniscus</i>	Q	D	K	H	E	E	D	Y	Q	L	M	Y	K	D	R	15
<i>Gorilla gorilla gorilla</i>	Q	D	K	H	E	E	D	Y	Q	L	M	Y	K	D	R	15
<i>Pongo abelii</i>	Q	D	K	H	E	E	D	Y	Q	L	M	Y	K	D	R	15
<i>Hylobates moloch</i>	Q	D	K	H	E	E	D	Y	Q	L	M	Y	K	D	R	15
<i>Mesocricetus auratus</i>	Q	D	K	Q	E	E	D	Y	Q	L	N	Y	K	D	R	13
<i>Phodopus campbelli</i>	Q	D	K	Q	E	E	D	Y	Q	L	N	Y	K	D	R	13
<i>Ovis aries</i>	Q	E	K	H	E	E	D	Y	Q	M	T	Y	K	D	R	12
<i>Panthera tigris altaica</i>	L	E	K	H	E	E	E	Y	Q	L	T	Y	K	D	R	11
<i>Felis catus</i>	L	E	K	H	E	E	E	Y	Q	L	T	Y	K	D	R	11
<i>Oryctolagus cuniculus</i>	L	E	K	Q	E	E	D	Y	Q	L	T	Y	K	D	R	11
<i>Canis lupus familiaris</i>	L	E	K	Y	E	E	E	Y	Q	L	T	Y	K	D	R	10
<i>Camelus dromedarius</i>	L	E	E	H	E	E	D	Y	Q	T	T	Y	K	D	R	10
<i>Canis lupus dingo</i>	L	E	K	Y	E	E	E	Y	Q	L	T	Y	K	D	R	10
<i>Sus scrofa domesticus</i>	L	E	K	L	E	E	D	Y	Q	I	T	Y	K	D	R	10
<i>Vicugna pacos</i>	L	K	E	H	E	E	D	Y	Q	A	I	Y	K	D	R	10
<i>Rhinolophus macrotis</i>	E	D	K	S	K	E	D	Y	E	L	N	Y	K	E	R	9
<i>Equus caballus</i>	L	E	K	S	E	E	E	H	Q	L	T	Y	K	D	R	9
<i>Equus przewalskii</i>	L	E	K	S	E	E	E	H	Q	L	T	Y	K	D	R	9
<i>Rhinolophus sinicus</i>	R	D	E	S	E	E	N	Y	Q	L	N	Y	K	E	R	9
<i>Rhinolophus ferrumequinum</i>	L	D	D	S	E	E	N	H	Q	L	N	F	K	E	R	7

Primate (*Pongo abelii*, *Nomascus leucogenys*, *Pan paniscus*, *Gorilla gorilla gorilla* and *Hylobates moloch*), golden hamster (*Mesocricetus auratus*), dwarf hamster (*Phodopus campbelli*), sheep (*Ovis aries*), tiger (*Panthera tigris altaica*), cat (*Felis catus*), rabbit (*Oryctolagus cuniculus*), dog (*Canis lupus familiaris* and *Canis lupus dingo*), camel (*Camelus dromedarius*), swine (*Sus scrofa domesticus*), alpaca (*Vicugna pacos*), horse (*Equus caballus* and *Equus przewalskii*) Chinese horseshoe bats (*Rhinolophus sinicus*), greater horseshoe bat (*Rhinolophus ferrumequinum*) and big-eared horseshoe bat (*Rhinolophus macrotis*)

**Table 2** Predicted hotspot residues and binding affinities (in Kd and  $\Delta G$ ) across the studied species

Species	31	41	83	353	Kd (nM)	$\Delta G$ (kcal mol <sup>-1</sup> )
<i>Canis lupus familiaris</i>	K	Y	Y	K	1.4	- 12.5
<i>Panthera tigris altaica</i>		Y	Y	K	1.5	- 12.5
<i>Camelus dromedarius</i>	E	Y	Y	K	1.6	- 12.5
<i>Canis lupus dingo</i>		Y	Y	K	1.6	- 12.5
<i>Felis catus</i>		Y	Y	K	1.7	- 12.4
<i>Phodopus campbelli</i>		Y	Y	K	1.8	- 12.4
<i>Ovis aries</i>		Y	Y	K	2.2	- 12.3
<i>Oryctolagus cuniculus</i>		Y	Y	K	2.3	- 12.2
<i>Pongo abelii</i>		Y	Y	K	2.3	- 12.2
<i>Mesocricetus auratus</i>		Y	Y	K	2.7	- 12.2
<i>Sus scrofa domesticus</i>		Y	Y	K	2.8	- 12.1
<i>Nomascus leucogenys</i>		Y	Y	K	2.9	- 12.1
<i>Pan paniscus</i>		Y	Y	K	3.0	- 12.1
<i>Rhinolophus sinicus</i>		Y	Y	K	3.0	- 12.1
<i>Gorilla gorilla gorilla</i>		Y	Y	K	3.1	- 12.1
<i>Homo sapiens</i>		Y	Y	K	3.1	- 12.1
<i>Hylobates moloch</i>		Y	Y	K	3.1	- 12.1
<i>Rhinolophus macrotis</i>		Y	Y	K	3.8	- 11.9
<i>Vicugna pacos</i>		Y	Y	K	3.8	- 11.9
<i>Equus caballus</i>			Y	K	6.1	- 11.4
<i>Equus przewalskii</i>			Y	K	6.1	- 11.4
<i>Rhinolophus ferrumequinum</i>			F	K	14.0	- 11.1

*Rhinolophus ferrumequinum*), *Homo sapiens*, and two species with equal affinity to humans (*Gorilla gorilla gorilla* and *Rhinolophus sinicus*) to assess their stability and further validate the predicted binding affinity scores. The simulation was run for 10 ns and the root mean square deviation (RMSD) of C-alpha atoms of all systems was determined (Fig. 1) to depict their dynamic stability as it measures the global fluctuations of proteins or complexes.

Compared to the RMSD value of *Homo sapiens* ACE2-RBD complex ( $2.05 \pm 0.44$  Å), the ACE2-RBD complex of *Canis lupus familiaris* ( $1.54 \pm 0.37$  Å), *Camelus dromedarius* ( $1.75 \pm 0.29$  Å) and *Panthera tigris altaica* ( $1.78 \pm 0.40$  Å) displayed lowest RMSD value, while the ACE2-RBD complex of *Rhinolophus ferrumequinum* ( $2.96 \pm 0.61$  Å), *Equus caballus* ( $2.71 \pm 0.46$  Å) and *Equus przewalskii* ( $2.61 \pm 0.46$  Å) displayed higher RMSD value. The RMSD value of ACE2-RBD complex of *Gorilla gorilla gorilla* ( $1.96 \pm 0.35$  Å) and *Rhinolophus sinicus* ( $1.90 \pm 0.28$  Å) was quite similar to that of *Homo sapiens*.

Overall, the results of the predicted binding affinities and complexes stability from MD simulations were consistent, which indicate that complexes from species that demonstrated higher binding affinities were slightly more stable than those which showed lower binding affinities during the course of the 10 ns trajectories. On the other hand, the species that showed similar binding affinities to *Homo sapiens* demonstrated also comparable stability during MD

simulation which further validates the predicted binding affinities.

Furthermore, to identify which residues play a pivotal role and contribute to the majority of the binding affinity, hotspots at ACE2/SARS-CoV-2-RBD interface were predicted (Table 2). As results, residues at position 31, 41, 83 and 353 in ACE2 proteins were identified as hotspots. The 83 and 353 hotspots were detected in all species, 41 was detected in 19 species and 31 only in 2 species. Remarkably, species that do not have a hotspot at position 41 have shown a higher Kd value (> 6) compared to the other species. The absence of hotspot at this position for these species may be due to substitution of tyrosine (Y) by histidine (H).

To validate this purpose, first we substituted Y by H in ACE2/RBD complex model of *Homo sapiens*, and inversely substituted H by Y in the complex model of *Rhinolophus ferrumequinum*, *Equus przewalskii* and *Equus caballus* and then recalculated the Kd value (Table 3). As a result, the substitution of Y by H in *Homo sapiens* model induces an increase in Kd value from 3.1 to 9.3 nM. In contrast, substitution of H by Y induces a decrease in Kd value from 14 to 4.8 nM for *Rhinolophus ferrumequinum* model and from 6.1 to 1.8 nM for *Equus przewalskii* and *Equus caballus*.

To understand how substitution of Y by H may affect the binding affinity, the binding mode of tyrosine 41 of *Homo sapiens* and histidine 41 of *Rhinolophus ferrumequinum* ACE2 in complex with RBD was studied (Fig. 2). As

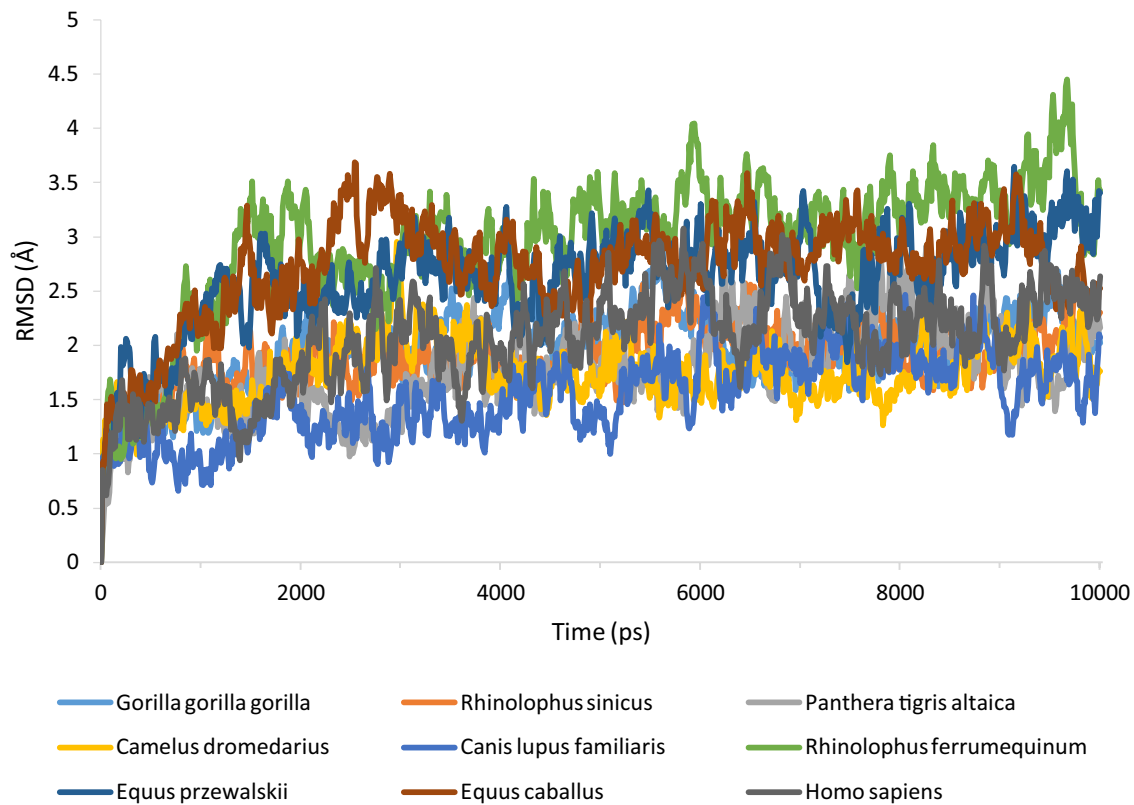


**Fig. 1** RMSD analysis of C-alpha atoms of the ACE2–RBD complexes of the studied species during 10 ns of MD simulations

**Table 3** Effect of H/Y substitution at position 41 on the binding affinity

Species	Wild type		Mutated*	
	Kd (nM)	$\Delta G$ (kcal mol <sup>-1</sup> )	Kd (nM)	$\Delta G$ (kcal mol <sup>-1</sup> )
<i>Homo sapiens</i>	3.1	– 12.1	9.3	– 11.4
<i>Rhinolophus ferromiquinum</i>	14.0	– 11.1	4.8	– 11.8
<i>Equus caballus</i>	6.1	– 11.4	1.8	– 12.4
<i>Equus przewalskii</i>	6.1	– 11.4	1.8	– 12.4

\*In *Homo sapiens* Y is substituted by H, and in the other species H is substituted by Y

indicated, in *Homo sapiens* ACE2–RBD complex, Tyrosine 41 by its hydroxyl group in the aromatic ring forms hydrogen bond with the oxygen atom of the side chain of the threonine at position 500 in RBD. In contrast, in *Rhinolophus ferromiquinum* complex, the imidazole side chain of histidine 41 does not dispose any hydroxyl group, and therefore cannot form a hydrogen bond with threonine 500 in RBD. Thus, substitution of Y by H may prevent the hydrogen-bonding interactions which consequently affect the binding affinity.

### Phylogenetic analysis

The phylogenetic tree was constructed to establish the correlation between the genetic distance and binding affinity.

As indicated in the phylogenetic tree (Fig. 3), no correlation between genetic distance and binding affinity was found, since some species with different affinities belong to the same branches while others with similar affinities are distributed in different branches.

### Discussion

The interaction of a virus with its host cell receptor is the first step in triggering a viral infection and is a key determinant of host cells and species range (Douam et al. 2015). In SARS-CoV-2, angiotensin-converting enzyme 2 (ACE2) was reported as the main host cell receptor and plays a

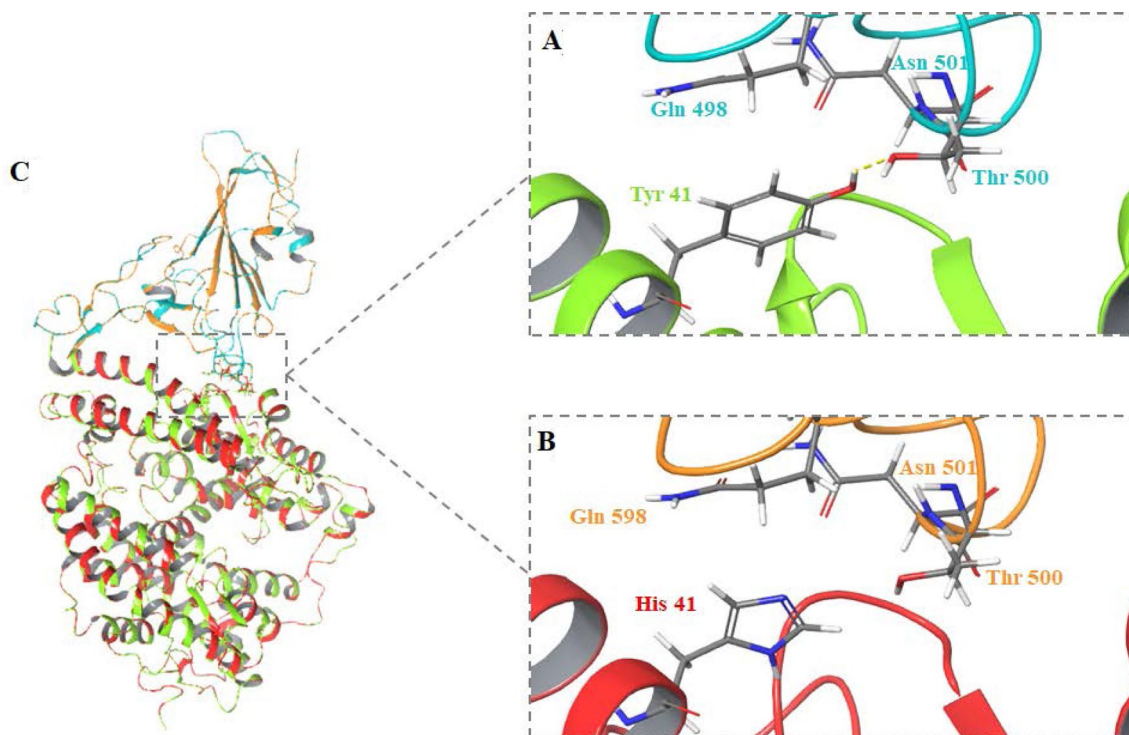


**Fig. 2** Effect of tyrosine/histidine substitution at 41 at the ACE2/SARS-CoV-2-RBD interface in *Homo sapiens* (a) and *Rhinolophus ferromiquinum* (b). The superimposed complexes of the both spe-

cies are indicated by cartoon representation (c). The hydrogen bond between Thr 500 and Tyr 41 is indicated by the yellow dashed line

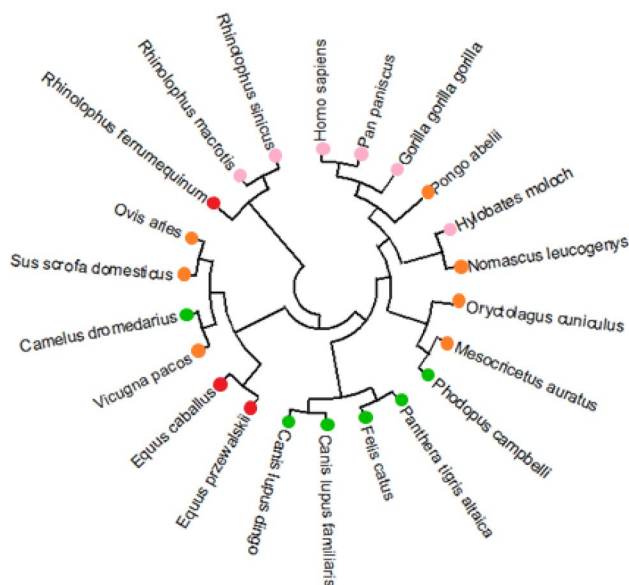


**Fig. 3** Phylogenetic tree of selected ACE2 orthologues showing the relation between genetic distance and the predicted ACE2–RBD Kd value. Red circles indicate species with a predicted ACE2–RBD Kd value more than 4, pink circles represent species with predicted ACE2–RBD Kd values between 3 and 4, orange circles represent species with predicted Kd values between 2 and 3, and green circles represents the species with predicted Kd values less than 2

crucial role in the recognition and entry of virus into cells to cause the final infection (Lu et al. 2020; Wan et al. 2020; Wrapp et al. 2020). The interaction between SARS-CoV-2 and hACE2 receptor is maintained by the viral spike protein (Chen et al. 2020). Although ACE2 is expressed in a large number of mammals, not all ACE2 can be used by SARS-CoV-2 as a host receptor (Qiu et al. 2020).

Here, we investigated ACE2 orthologues from 22 animals including forest, livestock and domestic animals to predict those with high susceptibility to SARS-CoV-2 by studying binding affinity and comparing the interaction mode between spike protein (through its RBD) and ACE2 from the studied species.

Our results predicted that the ACE2 receptor from animals such as dogs, tigers, camels, cats, dwarf hamsters and sheep have a slightly increased affinity to SARS-CoV-2-RBD compared to hACE2. However, animals like primates, rabbits, golden hamsters, swine, Chinese horseshoe bats, big-eared horseshoe bats and alpacas have an affinity approximate or equal to hACE2. However, three animals showed a slight decrease in affinity, including the two horse species and the greater horseshoe bat. The predicted binding affinities were further validated by MD simulations which showed that the stability of the ACE2–RBD complexes was correlated with increment and decrement of the binding affinity.

Our results further revealed that substitution of tyrosine by histidine at position 41 in ACE2 from the two species of horses and greater horseshoe bat could reduce their binding affinity to SARS-CoV-2-RBD.

Some species on our list of studied animals have already been reported as potential hosts for SARS-CoV-2. Experimental studies conducted by Shi et al. have shown that both dogs and cats are susceptible to infection with the virus; however, the viral replication was poor in dogs compared to cats (Shi et al. 2020). It has also been shown that SARS-CoV-2 was capable of using ACE2 from Chinese horseshoe bat and swine as an entry receptor (Zhou et al. 2020), which is consistent with our results as both species showed a binding affinity similar to that observed in hACE2.

Our results showed also that ACE2 from cats and tigers share a high similarity in their key contacting residues with SARS-CoV-2-RBD, which may indicate tigers as susceptible hosts for the virus. In fact, the first case of tiger COVID-19 was reported at the Bronx Zoo in New York City and it is believed that the infection was transmitted from an infected employee to the tiger.

Golden hamsters were also found to exhibit clinical and histopathological characteristics very similar to humans, making these species the most useful animal models for mimicking the human infection mechanisms of COVID-19 (Chan et al. 2020). Indeed, our data demonstrated that ACE2 from golden hamsters and dwarf hamsters showed comparable binding features with SARS-CoV-2-RBD, raising concerns for further investigation of dwarf hamsters as adequate animal models for SARS-CoV-2 infection. In another *in vitro* study, Liu et al. showed that sheep, rabbit and three primate species (*Pongo abelii*, *Nomascus leucogenys* and *Gorilla gorilla gorilla*) are susceptible to SARS-CoV-2 infection, which further validates our findings (Liu et al. 2020). These results from experimental and *in vivo* studies were consistent with our data which demonstrate the efficiency of *in silico* approaches in the prediction of SARS-CoV-2 host range.

The identification of animals with high susceptibility to SARS-Cov-2 remains essential to know the potential zoonotic reservoirs, particularly in livestock and domestic animals, which makes it possible to envisage epidemic surveillance of these animals to control the spread of the virus. This will also help to suggest animal models that could mimic human infection with SARS-CoV-2 to assist in the study of its pathogenicity and help in evaluating the efficacy and safety of new antiviral therapies and vaccines.

**Acknowledgements** This work was carried out under National Funding from the Moroccan Ministry of Higher Education and Scientific Research (COVID-19 Program) to AI. This work was also supported by a grant to AI from Institute of Cancer Research and the PPR-1 program to AI.

**Author contributions** El Mehdi Bouricha: conception and design of the work, data curation and analysis and original draft preparation. Mohammed Hakmi and Jihane Akachar: contributed in all stages of this research. Azeddine Ibrahim and Lahcen Belyamani: reviewed, edited and approved the version to be published.

## Compliance with ethical standards

**Conflict of interest** The authors declare that they have no competing interests.

**Ethical statements** This article does not contain any studies with human participants or animals performed by any of the authors.

## References

- Bowers, Kevin J., David E. Chow, Huafeng Xu, Ron O. Dror, Michael P. Eastwood, Brent A. Gregersen, John L. Klepeis, et al. 2006. "Scalable Algorithms for Molecular Dynamics Simulations on Commodity Clusters." In SC '06: Proceedings of the 2006 ACM/IEEE Conference on Supercomputing, 43–43. <https://doi.org/10.1109/SC.2006.54>.
- Chan J-W, Zhang AJ, Yuan S, Poon V-M, Chan C-S, Lee A-Y, Chan W-M et al (2020) Simulation of the clinical and pathological manifestations of coronavirus disease 2019 (COVID-19) in golden syrian hamster model: implications for disease pathogenesis and transmissibility. Clin Infect Dis. <https://doi.org/10.1093/cid/ciaa325>
- Chen Y, Guo Y, Pan Y, Zhao ZJ (2020) Structure analysis of the receptor binding of 2019-NCoV. Biochem Biophys Res Commun 525(1):135–140. <https://doi.org/10.1016/j.bbrc.2020.02.071>
- Cui J, Li F, Shi Z-L (2019) Origin and evolution of pathogenic coronaviruses. Nat Rev Microbiol 17(3):181–192. <https://doi.org/10.1038/s41579-018-0118-9>
- Douam F, Gaska JM, Winer BY, Ding Q, von Schaeuwen M, Ploss A (2015) Genetic dissection of the host tropism of human-tropic pathogens. Annu Rev Genet 49:21–45. <https://doi.org/10.1146/annurev-genet-112414-054823>
- Du L, Tai W, Zhou Y, Jiang S (2016) Vaccines for the prevention against the threat of MERS-CoV. Expert Rev Vaccines 15(9):1123–1134. <https://doi.org/10.1586/14760584.2016.1167603>
- Fehr AR, Perlman S (2015) Coronaviruses: an overview of their replication and pathogenesis. Methods Mol Biol 1282:1–23. [https://doi.org/10.1007/978-1-4939-2438-7\\_1](https://doi.org/10.1007/978-1-4939-2438-7_1)
- Humphrey W, Dalke A, Schulten K (1996) VMD: visual molecular dynamics. J Mol Graph 14(1):33–38. [https://doi.org/10.1016/0263-7855\(96\)00018-5](https://doi.org/10.1016/0263-7855(96)00018-5)
- Kirchdoerfer RN, Cottrell CA, Wang N, Pallesen J, Yassine HM, Turner HL, Corbett KS, Graham BS, McLellan JS, Ward AB (2016) Pre-fusion structure of a human coronavirus spike protein. Nature 531(7592):118–121. <https://doi.org/10.1038/nature17200>
- Kumar S, Stecher G, Li M, Knyaz C, Tamura K (2018) MEGA X: molecular evolutionary genetics analysis across computing platforms. Mol Biol Evol 35(6):1547–1549. <https://doi.org/10.1093/molbev/msy096>
- Lan J, Ge J, Jinfang Yu, Shan S, Zhou H, Fan S, Zhang Qi et al (2020) Structure of the SARS-CoV-2 spike receptor-binding domain bound to the ACE2 receptor. Nature. <https://doi.org/10.1038/s41586-020-2180-5>
- Liu Y, Gaowei Hu, Wang Y, Zhao X, Ji F, Ren W, Gong M et al (2020) Functional and genetic analysis of viral receptor ACE2 orthologs

- reveals a broad potential host range of SARS-CoV-2. *BioRxiv*. <https://doi.org/10.1101/2020.04.22.046565>
- Lu R, Zhao X, Li J, Niu P, Yang Bo, Honglong Wu, Wang W et al (2020) Genomic characterisation and epidemiology of 2019 novel coronavirus: implications for virus origins and receptor binding. *Lancet* (London, England) 395(10224):565–574. [https://doi.org/10.1016/S0140-6736\(20\)30251-8](https://doi.org/10.1016/S0140-6736(20)30251-8)
- Maestro, Schrödinger (2020). Maestro, Schrödinger, LLC, New York, NY, 2020;” 2020.
- Moreira IS, Koukos PI, Melo R, Almeida JG, Preto AJ, Schaarschmidt J, Trellet M, Gümüş ZH, Costa J, Bonvin AMJJ (2017) Spoton: high accuracy identification of protein-protein interface hot-spots. *Sci Rep* 7(1):8007. <https://doi.org/10.1038/s41598-017-08321-2>
- Peiris, J. S. M. 2012. “57 - Coronaviruses.” In *Medical Microbiology (Eighteenth Edition)*, edited by David Greenwood, Mike Barer, Richard Slack, and Will Irving, 587–93. Edinburgh: Churchill Livingstone. <https://doi.org/https://doi.org/10.1016/B978-0-7020-4089-4.00072-X>.
- Pettersen EF, Goddard TD, Huang CC, Couch GS, Greenblatt DM, Meng EC, Ferrin TE (2004) UCSF chimera—a visualization system for exploratory research and analysis. *J Comput Chem* 25(13):1605–1612. <https://doi.org/10.1002/jcc.20084>
- Qiu Ye, Zhao Y-B, Wang Q, Li J-Y, Zhou Z-J, Liao C-H, Ge X-Y (2020) Predicting the angiotensin converting enzyme 2 (ACE2) utilizing capability as the receptor of SARS-CoV-2. *Microbes Infect*. <https://doi.org/10.1016/j.micinf.2020.03.003>
- Shang J, Ye G, Shi Ke, Wan Y, Luo C, Aihara H, Geng Q, Auerbach A, Li F (2020) Structural basis of receptor recognition by SARS-CoV-2. *Nature*. <https://doi.org/10.1038/s41586-020-2179-y>
- Shi J, Wen Z, Zhong G, Yang H, Wang C, Huang B, Liu R et al (2020) Susceptibility of ferrets, cats, dogs, and other domesticated animals to SARS–coronavirus 2. *Science*. <https://doi.org/10.1126/science.abb7015>
- Sievers F, Wilm A, Dineen D, Gibson TJ, Karplus K, Li W, Lopez R et al (2011) Fast, scalable generation of high-quality protein multiple sequence alignments using clustal omega. *Mol Syst Biol* 7(October):539. <https://doi.org/10.1038/msb.2011.75>
- Song W, Gui M, Wang X, Xiang Ye (2018) Cryo-EM structure of the SARS coronavirus spike glycoprotein in complex with its host cell receptor ACE2. *PLoS Pathog* 14(8):e1007236. <https://doi.org/10.1371/journal.ppat.1007236>
- Vangone A, Bonvin AMJJ (2015) “Contacts-based prediction of binding affinity in protein-protein complexes” edited by Michael Levitt. *ELife* 4:e07454. <https://doi.org/10.7554/eLife.07454>
- Walls AC, Young-Jun Park M, Tortorici A, Wall A, McGuire AT, Veesler D (2020) Structure, function, and antigenicity of the SARS-CoV-2 spike glycoprotein. *Cell* 181(2):281–292.e6. <https://doi.org/10.1016/j.cell.2020.02.058>
- Wan Y, Shang J, Graham R, Baric RS, Li F (2020) Receptor recognition by the novel coronavirus from Wuhan: an analysis based on decade-long structural studies of SARS coronavirus. *J Virol* 94(7):e00127–e220. <https://doi.org/10.1128/JVI.00127-20>
- Wang N, Shang J, Jiang S, Lanying Du (2020) Subunit vaccines against emerging pathogenic human coronaviruses. *Front Microbiol* 11:298. <https://doi.org/10.3389/fmicb.2020.00298>
- Waterhouse A, Bertoni M, Bienert S, Studer G, Tauriello G, Gumienny R, Heer FT et al (2018) SWISS-MODEL: homology modelling of protein structures and complexes. *Nucleic Acids Res* 46(W1):W296–303. <https://doi.org/10.1093/nar/gky427>
- Waterhouse AM, Procter JB, Martin DMA, Clamp M, Barton GJ (2009) Jalview version 2—a multiple sequence alignment editor and analysis workbench. *Bioinformatics* 25(9):1189–1191. <https://doi.org/10.1093/bioinformatics/btp033>
- Wrapp D, Wang N, Corbett KS, Goldsmith JA, Hsieh C-L, Abiona O, Graham BS, McLellan JS (2020) Cryo-EM structure of the 2019-NCoV spike in the prefusion conformation. *Science* 367(6483):1260–1263. <https://doi.org/10.1126/science.abb2507>
- Xue LC, Rodrigues JP, Kastiris PL, Bonvin AM, Vangone A (2016) PRODIGY: a web server for predicting the binding affinity of protein-protein complexes. *Bioinformatics* 32(23):3676–3678. <https://doi.org/10.1093/bioinformatics/btw514>
- Yan R, Zhang Y, Yaning Li Lu, Xia YG, Zhou Q (2020) Structural basis for the recognition of SARS-CoV-2 by full-length human ACE2. *Science* 367(6485):1444–1448. <https://doi.org/10.1126/science.abb2762>
- Yuan Y, Cao D, Zhang Y, Ma J, Qi J, Wang Q, Guangwen Lu et al (2017) Cryo-EM structures of MERS-CoV and SARS-CoV spike glycoproteins reveal the dynamic receptor binding domains. *Nature Commun* 8:15092. <https://doi.org/10.1038/ncomms15092>
- Zhou P, Yang X-L, Wang X-G, Ben Hu, Zhang L, Zhang W, Si H-R et al (2020) A pneumonia outbreak associated with a new coronavirus of probable bat origin. *Nature* 579(7798):270–273. <https://doi.org/10.1038/s41586-020-2012-7>